Manuscript for *The Holocene* (Research Report)

High-latitude fire activity of recent decades derived from microscopic charcoal and black carbon in Greenland ice cores

Sandra O. Brugger^{1,*}, Nathan J. Chellman¹, Callie McConnell², Joseph R. McConnell¹

Abstract

Warming temperatures and prolonged drought periods cause rapid changes of fire frequencies and intensities in high-latitude ecosystems. Associated smoke plumes deposit dark particles from incomplete combustion on the Greenland ice sheet that reduce albedo but also provide a detailed record of paleofire history. Here, we apply an emerging microscopic charcoal technique in combination with established black carbon and lead pollution measurements to an array of ten ice cores from southern to central Greenland that span recent decades. We found that microscopic charcoal deposition is highly variable among sites, with a few records suggesting recently increasing fire activity possibly in response to growing fire activity in boreal forest ecosystems. This stands in contrast to decreasing trends in black carbon measured in the same ice cores, consistent with contributions from industrial fossil fuel emissions. Decreasing trends of lead pollution and occurrence of microscopic spheroidal carbonaceous particles (SCP), a microfossil tracer of fossil fuel emissions, further support our interpretation that black carbon in this region is influenced by industrial emissions during recent decades. We conclude that microscopic charcoal analyses in ice may help disentangle biomass burning from fossil-fuel emissions during the industrial period and have potential to contribute to better understanding of regional high-latitude fire regimes.

Keywords: Black carbon, ice core, lead, microscopic charcoal, paleofire, SCP (spheroidal carbonaceous particles)

¹ Division of Hydrologic Sciences, Desert Research Institute, Reno, NV, USA

² U.S. Forest Service, WO Detached Unit, Corvallis, Oregon

^{*} Corresponding author

1 Introduction

Rapid climate change during recent decades has resulted in pronounced changes of biomass burning (Bowman et al., 2009), especially in high latitudes of the Northern Hemisphere (e.g., Feurdean et al., 2021; Novenko et al., 2022; Pan et al., 2011; Randerson et al., 2006) where surface temperatures are rising twice as fast as the global mean (Dai et al., 2019; Serreze and Francis, 2006). Such fires in the boreal-tundra ecotone and adjacent boreal forests may lead to further warming via positive feedback mechanisms. For example, the deposition of light absorbing black carbon particles on Arctic snow decreases snow surface albedo, leads to earlier snowmelt (Stohl et al., 2006), and in turn contributes to further warming and increasing fire risks (Pan et al., 2011). Greenland ice cores provide a continental to hemispheric record of past climate and environmental dynamics (e.g., Grieman et al., 2018; Legrand et al., 2016; McConnell et al., 2018, 2019; Rasmussen et al., 2014; Seierstad et al., 2014; Sigl et al., 2015; Vinther et al., 2010) and preserve many different indicators of past biomass burning activity (e.g., Kang et al., 2020; Kehrwald et al., 2020; Legrand et al., 2016; Liu et al., 2021; Nicewonger et al., 2020; McConnell et al., 2007; Zennaro et al., 2014). However, some burning proxies such as black carbon cannot be strictly interpreted as biomass burning indicators during the industrial period as they contain an increasingly dominant component from fossil fuel and other anthropogenic emissions potentially overshadowing the biomass burning signal (McConnel et al., 2007). Microscopic charcoal is a proxy specific to biomass burning that is not impacted by industrial emissions (Reese et al., 2013), and recent methodical advancements allow for microscopic charcoal measurements at extremely low concentrations in Greenland ice (Brugger et al., 2018). The first Greenland ice-core record of microscopic charcoal was derived from Summit (Eurocore'89) and while the record does not extend to present, it indicates a possible increase in fire activity in the late 20th century (Brugger et al., 2019). Thus, we hypothesize that Greenland ice cores reflect the increased fire risks in high-latitude ecosystems in recent decades because of a warming and drying climate (e.g., McCarty et al., 2021; Pan et al., 2011). Using an array of ice cores from southern and central Greenland, here we investigate 1) if large-scale fire activity has increased during recent decades in response to warming temperatures using a combination of biomass-burning-specific microscopic charcoal and established black carbon measurements, and 2) if sites show regionally varying patterns in charcoal deposition due to the potentially shorter atmospheric lifetime of these large (micronsize) particles compared to submicron-sized black carbon.

2 Material and methods

We used an array of ten ice core sites spanning a wide altitudinal (2120m a.s.l. to 3232m a.s.l.), latitudinal (62.2°N to 72.4°N), and longitudinal (36.2°W to 46.3°W) gradient across southern and central Greenland. The array consists of seven short firn cores that were retrieved in 2003 and 2004, hereafter referred to as Basin cores 1 to 2 and 4 to 8 (Hanna et al., 2006). Additionally, we included the shallow sections of ice cores from ACT11c (unpublished) and ACT11d (McConnell et al. 2019; Mernild et al. 2015), drilled in 2011, as well as the published microscopic charcoal record from the Summit area (Eurocore'89; Brugger et al., 2019). Some of the lower-elevation Basin cores in southern Greenland were impacted by melt events as indicated by ice lenses, especially the southernmost core from Basin 4. However, these ice lenses span at most several centimeters of depth, and thus do not significantly impact the decadal-scale trends targeted by this study. Table 1 provides further details on the individual ice cores.

We conducted black carbon measurements using a Single Particle Soot Photometer (SP2) (McConnell et al., 2007) and lead measurements among other chemical species using Inductively-Coupled Plasma-Mass-Spectrometry (ICP-MS) as part of the continuous ice-core-analytical system hosted at Desert Research Institute, Nevada (McConnell et al. 2019, 2021). We used black carbon as a tracer for fossil fuel and biomass burning (McConnell et al. 2007) and lead as an additional proxy for general industrial pollution (i.e., McConnell et al. 2019). The chronologies were established using annual layer counting of black carbon, sulfur, sodium, calcium, and stable water isotopes.

For the Basin cores, meltwater samples for microscopic charcoal analyses were collected in 1L polyethylene jars as part of the continuous flow analysis. An exotic marker tablet (i.e., *Lycopodium*, batch # 3862 with 9666±671 (1σ) spores per tablet) was added immediately to each sample following standard practice (Brugger et al., 2018). For the ACT11c and ACT11d cores, ice samples were cut directly from the archived ice cores, melted in 1L polyethylene jars, and spiked with the same marker tablet. We extracted microfossils following Brugger et al. (2018), including evaporation of the samples at ca. 70 °C to reduce the initial water volume, followed by a chemical treatment with acetolysis. We added an additional hydrofluoric acid (40% HF) treatment to reduce abundant dust content following the methods in Brugger et al. (2019) for Greenland samples. Finally, we mounted the samples in glycerol for optical determination of microfossils. Microscopic charcoal analysis was conducted with a light

microscope at 40x magnification using established determination criteria (Tinner and Hu, 2003) and minimum counting sums of 200 *Lycopodium* spores plus charcoal fragments and until each group consisted of minimum 20 items. (Finsinger and Tinner, 2005). Additionally, we used spheroidal carbonaceous particles (SCP) as a specific tracer for fossil fuel emissions (Rose, 2015).

Fluxes were calculated using the annual accumulation rate from each site based on ice layer counting, with average deposition rates determined by the mean of the samples from each core weighted by the number of years represented by individual samples. Because of sampling volume constraints, the microfossil samples have differing depth resolutions and record lengths, leading to inconsistent temporal overlap between all ten ice cores (Table 1). The annual resolution of the black carbon and lead records allowed for evaluation of annual deposition between 1990-2000 CE for all sites. We used correlation analyses between sites and proxies to establish relationships among the three indicators.

3 Results

Microscopic charcoal concentrations are highly variable for all sites and range between \sim 200 to 400 fragments L⁻¹ except for Summit (Supplementary figure S1). In three out of four Summit samples covering the period post-1950 CE, concentrations are as high as \sim 1400 fragments L⁻¹. This discrepancy between Summit and the lower-elevation sites can be explained by the relatively low snow accumulation rate at Summit (\sim 0.2 m y⁻¹) compared to the other sites (\sim 0.4-1.2 m y⁻¹; see Supplementary figure S4).

Similarly, microscopic charcoal depositional flux is highly variable and shows no clear temporal trend between sites, suggesting that different source regions of forest fire emissions contribute to the signal at individual sites (Figure 1). However, the microscopic charcoal flux values are elevated in the topmost samples from Basin cores 2 (300,000 fragments m⁻² y⁻¹), 4 (100,000 fragments m⁻² y⁻¹), 5 (200,000 fragments m⁻² y⁻¹), 7 (260,000 fragments m⁻² y⁻¹), and 8 (180,000 fragments m⁻² y⁻¹) for the period 2000-2003 CE. Also, ACT11d suggests a two-fold increase of microscopic charcoal influx to >200,000 fragments m⁻² y⁻¹ in the topmost sample compared to the previous 60 years of the record. ACT11c and Basin 6 only consist of three and four samples covering the period 2000-2011 CE and 1985-2003 CE, respectively. However, microscopic charcoal fluxes in these recent samples are similarly high compared to the nearby ACT11d site. Thus, most of the individual microscopic charcoal records point to increased fire

activity in the recent decades compared to the second half of the 20^{th} century (Figure 1), with the exception of Basin 1 where the two samples suggest declining fire activity towards present with counts of \sim 6,000 fragments m-2 y-1 and below detection limits (0 fragments were found in a water equivalent sample volume of 366 g).

Decadal values of black carbon fluxes for most sites are ~0.25-0.5 ng m⁻² y⁻¹ except for the two neighboring sites ACT11c and ACT11d where black carbon fluxes reach up to 1 and 2 ng m⁻² y⁻¹, respectively (Figure 1). Black carbon deposition is relatively constant at Basin 1, 2, 6, 7, and 8, but decreases to present in Basin cores 4 and 5, ACT11c, ACT11d, and Summit (Figure 1). Black carbon fluxes for individual years reach up to 4.5 ng m⁻² y⁻¹ in 1977 CE in the ACT11c core and 2.5 ng m⁻² y-1 in 1967 CE in Basin core 5 (Supplementary figures S2-S11). In the Summit record, major peaks in black carbon influx in 1951 and 1976/1984 CE correlate with increased microscopic charcoal influx during 1950-1955 CE and 1970-1989 CE, respectively. Similarly, the years with highest peaks of black carbon in the Basin 2 and Basin 6 records correlate with enhanced charcoal influx in the corresponding sample period.

Decadal lead fluxes are around ~0.025 ng m⁻² y⁻¹ at Basin 1, 2, 6, 7, 8, and Summit and up to 0.1 ng m⁻² y⁻¹ at Basin 4, Basin 5, ACT11c and ACT11d (Figure 1), indicating that a larger amount of lead pollution reaches the more southerly sites. All ten lead records decrease to present, suggesting that overall industrial pollution has decreased in recent decades. Single finds of SCP were present in at least one microfossil sample from the ice core sites ACT11c, ACT11d, Summit, Basin 1, 2, 5, and 6, despite the relatively small ice sample volumes (Supplementary figures S2-S11), suggesting that micron-size pollution particles from fossil fuel combustion reached the remote Greenland ice sheet, though the sparse SCP finds preclude evaluation of temporal trends

The spatial distribution of microscopic charcoal, black carbon, and lead influx (Figure 2) suggests that sites with higher microscopic charcoal influx generally receive more black carbon and lead. The neighboring low-elevation sites in East Greenland, including Basin 6, Basin 7 and ACT11c sites have influx values of ~200,000 microscopic fragments m⁻² y⁻¹, black carbon fluxes of ~0.4 to 1.3 ng m⁻² y⁻¹, and are among the cores with higher lead values. Likewise, the ice cores sites with lower influx of microscopic charcoal generally have lower deposition of black carbon and lead (Figure 2). While black carbon and lead deposition are significantly correlated (p-level<0.01; Figure 3), the correlation of microscopic charcoal with black carbon (Figure 3) or with lead is not significant (p-level>0.1).

4 Discussion

Traditional microscopic charcoal records from lake sediments reflect fire activity in a maximum area of few hundred kilometers due to the relatively short atmospheric lifetime of these larger particles (Adolf et al., 2018). However, the Arctic biome closest to the ice core sites is generally characterized by low fire activity although it experienced wildfires recently (Evangeliou et al., 2019; McCarty et al., 2021). Therefore, most microscopic charcoal found in Greenland ice cores probably derives from the numerous large forest fires in the boreal forest belt— climatically restricted to ca. 42° to 71° N and over 1000 km from our ice core sites (Pfadenhauer and Klötzli, 2015), suggesting that at least some microscopic charcoal particles can be transported over long distances.

Pronounced year-to-year variability in fire activity and transport are likely more important than longer-term trends across the boreal biome in determining deposition of charcoal on the ice sheet. Our finding is in agreement with findings from local sediment charcoal records across high-latitude ecosystems in North America (Hoecker et al., 2020), and consistent with FLEXPART emission sensitivity modelling (e.g., McConnell et al., 2019) indicating that low-elevation sites such as used in this study are sensitive to smaller geographical areas than high-elevation sites. Nevertheless, some of the charcoal records contain peak values in the topmost samples, suggesting that overall boreal forest fire activity or fire frequencies probably increased during recent decades (Hoecker et al. 2020).

Black carbon deposition shows a decreasing trend overall, similar to longer published black carbon records from Arctic ice cores (e.g., Bauer et al., 2013; Du et al. 2020; Kang et al., 2020; McConnell et al., 2007; Osmont et al. 2019) but contrasting with microscopic charcoal counts that increase towards present. Basin 1, where fluxes for both tracers decline in the topmost samples, is the exception. Since black carbon deposition may include significant contributions from fossil fuel emissions (Bond et al., 2013, McConnell et al. 2007), it probably is not representative solely of biomass burning during this period (i.e., industrial period) in contrast to microscopic charcoal that derives only from biomass burning. Thus, the decreasing black carbon trends are likely driven by decreasing fossil fuel emissions across North America and Europe during recent decades (e.g., Du et al., 2020; Hoesly et al., 2018). Single finds of SCP also suggest that fossil fuel pollution continues to impact the Greenland ice sheet during this period (e.g., Hicks and Isaksson, 2006; Rose, 2015). In parallel to black carbon, decreasing lead deposition since 1970 CE provides further evidence that the black carbon signal may be

influenced by industrial pollution rather than forest fires in agreement with other pollution indicators derived from Arctic ice cores (Geng et al., 2014; McConnell and Edwards, 2008).

However, some black carbon records from ice cores within the Alaskan and Canadian boreal forests suggest regionally increasing black carbon deposition after the 1980s and 2000s, respectively, which has been attributed partly to increasing forest fire activity (Neff et al., 2012; Sierra-Hernández et al., 2022), and may be reflecting similar wild-fire dominated sources from within the boreal forest biome as captured in our remote microscopic charcoal records.

The large black carbon deposition in individual years, and corresponding enhanced charcoal deposition of the same decade suggests that larger fire events may have increased transport efficiency for smoke plumes, and together with beneficial atmospheric conditions, may have resulted in proportionally larger microscopic charcoal deposition as well as black carbon (Thomas et al., 2017). Similarly, previous vanillic acid-based fire records, a specific tracer for conifer combustion, suggest massive, short burning periods rather than long-term trends in fire activity (McConnell et al. 2007).

Our array of ice cores suggests a strong spatial gradient with high deposition in low-elevation East Greenland for all three impurities— microscopic charcoal, black carbon, and lead. Significant deposition of black particles on the Greenland ice sheet may ultimately result in changes of the snow surface albedo (Cordero et al. 2022; Doherty et al. 2010; Kang et al., 2020; Stohl, 2006) and induce feedback mechanisms with warming climate that in turn may result in more frequent high-latitude forest fires (Bond et al., 2013).

5 Conclusions

Large particles emitted from biomass burning such as microscopic charcoal are not transported as far as the submicron-size fire tracers typically used in ice cores, meaning that the microscopic-charcoal records in the array likely provide paleoinformation on regional high-latitude fire activity immediately west of Greenland.

Incorporating microscopic charcoal as a specific burning tracer for biomass burning gives new insights into the burning sources of fire records from Greenland ice cores during the industrial period. Microscopic charcoal shares a common spatial pattern with black carbon (i.e., a South to North gradient) but temporal trends over the past decades are different. Previous black carbon studies suggest that fossil fuel contributions to black carbon have been decreasing over the past decades. Thus, we hypothesize that decreasing emission of black carbon from fossil-fuel

burning offset increasing emissions from biomass burning in recent decades, while the biomass-burning specific microscopic charcoal fluxes suggest rising fire activity in the source regions immediately west of Greenland. This is in agreement with remote sensing information showing prolonged fire seasons in response to climate warming and drying during recent decades. More widely distributed multiproxy biomass burning records that include charcoal and encompassing longer timespans are needed to monitor the geographic distribution of high-latitude forest fires and their impacts. Such information on Greenland snow impurities is crucial to understand feedback mechanisms of climate warming, forest fires, and Greenland ice sheet melting processes.

6 Acknowledgements

We acknowledge NASA and NSF grants NAG5-12752 and 0909499 to J.R. McConnell for funding collection and analyses of the Basin and ACT (11c and 11d) cores, respectively. We thank the drilling teams for collecting the array of ice cores over several fieldwork seasons at the different ice core sites. This microfossil study was funded by the Swiss National Science Foundation (SNSF Early Postdoc.Mobility grant P2BEP2 188180).

7 References

Adolf C, Wunderle S, Colombaroli D et al. (2018) The sedimentary and remote-sensing reflection of biomass burning in Europe. *Global Ecology and Biogeography* 27: 199–212.

Bauer SE, Bausch A, Nazarenko L et al. (2013) Historical and future black carbon deposition on the three ice caps: Ice core measurements and model simulations from 1850 to 2100. *Journal of Geophysical Research: Atmospheres* 118: 7948–7961.

Bond TC, Doherty SJ, Fahey DW et al. (2013) Bounding the role of black carbon in the climate system: A scientific assessment. *Journal of Geophysical Research: Atmospheres* 118: 5380–5552.

Bowman DM, Balch JK, Artaxo P et al. (2009) Fire in the Earth system. Science 324: 481–484.

Brugger SO, Gobet E, Blunier T et al. (2019) Palynological insights into global change impacts on Arctic vegetation, fire, and pollution recorded in Central Greenland ice. *The Holocene*, 29: 1189–1197.

- Brugger SO, Gobet E, Schanz FR et al. (2018) A quantitative comparison of microfossil extraction methods from ice cores. *Journal of Glaciology* 64: 432–442.
- Cordero RR, Sepúlveda E, Feron S. et al. (2022) Black carbon footprint of human presence in Antarctica. *Nature communications* 13. https://doi.org/10.1038/s41467-022-28560-w
- Dai A, Luo D, Song M et al. (2019) Arctic amplification is caused by sea-ice loss under increasing CO 2. *Nature communications* 10: 1–13.
- Doherty SJ, Warren SG, Grenfell TC et al. (2010) Light-absorbing impurities in Arctic snow. *Atmospheric Chemistry and Physics* 10: 11647–11680.
- Evangeliou N, Kylling A, Eckhardt S et al. (2019) Open fires in Greenland in summer 2017: transport, deposition and radiative effects of BC, OC and BrC emissions. *Atmospheric Chemistry and Physics* 19: 1393–1411.
- Feurdean A, Diaconu A-C, Pfeiffer M et al. (2021) Holocene wildfire regimes in forested peatlands in western Siberia: interaction between peatland moisture conditions and the composition of plant functional types. *Climate of the Past Discussion*. https://doi.org/10.5194/cp-2021-125.
- Finsinger W, Tinner W (2005) Minimum count sums for charcoal concentration estimates in pollen slides: accuracy and potential errors. *The Holocene* 15: 293–297.
- Geng L, Alexander B, Cole-Dai J, Steig EJ et al. (2014) Nitrogen isotopes in ice core nitrate linked to anthropogenic atmospheric acidity change. *Proceedings of the National Academy of Sciences* 111: 5808–5812.
- Grieman MM, Aydin M, McConnell JR, Saltzman ES (2018) Burning-derived vanillic acid in an Arctic ice core from Tunu, northeastern Greenland. *Climate of the Past* 14: 1625–1637.
- Hanna E, McConnell JR, Das S et al. (2006) Observed and modeled Greenland ice sheet snow accumulation, 1958–2003, and links with regional climate forcing. *Journal of Climate* 19: 344–358.

- Hicks S, Isaksson E (2006) Assessing source areas of pollutants from studies of fly ash, charcoal, and pollen from Svalbard snow and ice. *Journal of Geophysical Research* 111: D02113.
- Hoecker TJ, Higuera PE, Kelly R, Hu FS (2020) Arctic and boreal paleofire records reveal drivers of fire activity and departures from Holocene variability. *Ecology* 101: e03096.
- Hoesly RM, Smith SJ, Feng L et al. (2018) Historical (1750–2014) anthropogenic emissions of reactive gases and aerosols from the Community Emissions Data System (CEDS). *Geoscientific Model Development* 11: 369–408.
- Kang S, Zhang Y, Qian Y, Wang H (2020) A review of black carbon in snow and ice and its impact on the cryosphere. *Earth-Science Reviews* 210: 103346.
- Kehrwald NM, Jasmann JR, Dunham ME et al. (2020) Boreal blazes: biomass burning and vegetation types archived in the Juneau Icefield. *Environmental Research Letters* 15: 085005.
- Legrand M, McConnell J, Fischer H et al. (2016) Boreal fire records in Northern Hemisphere ice cores: a review. *Climate of the Past* 12: 2033–2059.
- Liu P, Kaplan JO, Mickley LJ et al. (2021) Improved estimates of preindustrial biomass burning reduce the magnitude of aerosol climate forcing in the Southern Hemisphere. *Science Advances* 7: eabc1379.
- McCarty JL, Aalto J, Paunu VV et al. (2021) Reviews and syntheses: Arctic fire regimes and emissions in the 21st century. *Biogeosciences* 18: 5053–5083.
- McConnell JR, Chellman NJ, Wilson AI et al. (2019) Pervasive Arctic lead pollution suggests substantial growth in medieval silver production modulated by plague, climate, and conflict. *Proceedings of the National Academy of Sciences* 116: 14910–14915.
- McConnell JR, Edwards R, Kok GL et al. (2007) 20th-century industrial black carbon emissions altered arctic climate forcing. *Science* 317: 1381–1384.

- McConnell JR, Edwards R (2008) Coal burning leaves toxic heavy metal legacy in the Arctic. Proceedings of the National Academy of Sciences 105: 12140–12144.
- McConnell JR, Wilson AI, Stohl A et al. (2018) Lead pollution recorded in Greenland ice indicates European emissions tracked plagues, wars, and imperial expansion during antiquity. *Proceedings of the National Academy of Sciences* 115: 5726–5731.
- Mernild SH, Hanna E, McConnell JR et al. (2015) Greenland precipitation trends in a long-term instrumental climate context (1890–2012): Evaluation of coastal and ice core records. *International Journal of Climatology* 35: 303–320.
- Neff PD, Steig EJ, Clark DH et al. (2012) Ice-core net snow accumulation and seasonal snow chemistry at a temperate-glacier site: Mount Waddington, southwest British Columbia, Canada. *Journal of Glaciology* 58: 1165-1175.
- Nicewonger MR, Aydin M, Prather MJ, Saltzman ES (2020) Extracting a History of Global Fire Emissions for the Past Millennium From Ice Core Records of Acetylene, Ethane, and Methane. *Journal of Geophysical Research: Atmospheres* 125: e2020JD032932.
- Novenko EY, Kupryanov DA, Mazei NG et al. (2022) Evidence that modern fires may be unprecedented during the last 3400 years in permafrost zone of central Siberia, Russia. *Environmental Research Letters* 17: 025004.
- Osmont D, Wendl IA, Schmidely L et al. (2018) An 800-year high-resolution black carbon ice core record from Lomonosovfonna, Svalbard. *Atmospheric Chemistry and Physics* 18: 12777–12795.
- Pan Y, Birdsey RA, Fang J et al. (2011) A large and persistent carbon sink in the world's forests. *Science* 333: 988–993.
- Pfadenhauer JS, Klötzli FA (2015) Vegetation der Erde: Grundlagen, Ökologie, Verbreitung. Berlin-Heidelberg: Springer.
- Randerson JT, Liu H, Flanner MG et al. (2006) The impact of boreal forest fire on climate warming. *Science* 314: 1130–1132.

- Rasmussen SO, Bigler M, Blockley SP et al. (2014) A stratigraphic framework for abrupt climatic changes during the Last Glacial period based on three synchronized Greenland ice-core records: refining and extending the INTIMATE event stratigraphy. *Quaternary Science Reviews* 106: 14–28.
- Reese CA, Liu KB, Thompson LG (2013) An ice-core pollen record showing vegetation response to Late-glacial and Holocene climate changes at Nevado Sajama, Bolivia. *Annals of Glaciology* 54: 183-190.
- Rose NL (2015) Spheroidal carbonaceous fly ash particles provide a globally synchronous stratigraphic marker for the Anthropocene. *Environmental Science & Technology* 49: 4155–4162.
- Seierstad IK, Abbott PM, Bigler M et al. (2014) Consistently dated records from the Greenland GRIP, GISP2 and NGRIP ice cores for the past 104 ka reveal regional millennial-scale δ18O gradients with possible Heinrich event imprint. *Quaternary Science Reviews* 106: 29–46.
- Serreze MC, Francis JA (2006) The Arctic amplification debate. Climatic change 76: 241–264.
- Sierra-Hernández MR, Beaudon E, Porter SE et al. (2022) Increased Fire Activity in Alaska since the 1980s: Evidence from an Ice Core-derived Black Carbon Record. *Journal of Geophysical Research: Atmospheres* 127: e2021JD035668.
- Sigl M, Winstrup M, McConnell JR et al. (2015) Timing and climate forcing of volcanic eruptions for the past 2,500 years. *Nature* 523: 543–549.
- Stohl A (2006) Characteristics of atmospheric transport into the Arctic troposphere. *Journal of Geophysical Research: Atmospheres* 111: D11306.
- Thomas JL, Polashenski CM, Soja AJ et al. (2017) Quantifying black carbon deposition over the Greenland ice sheet from forest fires in Canada. *Geophysical Research Letter*, 44: 7965–7974.
- Tinner W, Hu FS (2003) Size parameters, size-class distribution and area-number relationship of microscopic charcoal: relevance for fire reconstruction. *The Holocene* 13: 499–505.

Vinther BM, Jones PD, Briffa KR et al. (2010) Climatic signals in multiple highly resolved stable isotope records from Greenland. *Quaternary Science Reviews* 29: 522–538.

Zennaro P, Kehrwald N, McConnell JR et al. (2014) Fire in ice: two millennia of boreal forest fire history from the Greenland NEEM ice core. *Climate of the Past* 10: 1905–1924.

8 Figures and tables

Table 1. Details on ice core sites used for this study.

(Code) Site	Drilling year	Location	Altitude (m a.s.l.)	Core length (m)	Age (Year CE)	Publication	Microfossil samples	Sample volume range (average) (g)
(d) ACT11d	2011	66.5°N 46.3°W	2120	35.31	1950-2011	Mernild et al. (2015)	7	1729-7299 (3856)
(c) ACT11c	2011	66.3°N 40.7°W	2077	20.36	2000-2011	Unpublished	3	2591-4317 (3704)
(S) Summit Eurocore'89	1989	72.4°N 37.4°W	3232	18.97	1950-1989	Brugger et al. (2018)	4	1090-2357 (1848)
(1) Basin 1	2004	71.5°N 42.3°W	2971	20,3	1976-2004	Hanna et al. (2006)	5	233-613 (399)
(2) Basin 2	2003	68.2°N 44.5°W	2224	17	1980-2003	Hanna et al. (2006)	3	345-753 (590)
(4) Basin 4	2004	62.2°N 46.2°W	2350	24	1973-2004	Hanna et al. (2006)	4	401-864 (665)
(5) Basin 5	2003	63.6°N 46.2°W	2520	24	1964-2003	Hanna et al. (2006)	5	205-830 (641)
(6) Basin 6	2003	66.6°N 41.4°W	2467	24,5	1983-2003	Hanna et al. (2006)	5	304-742 (584)
(7) Basin 7	2003	67.3°N 40.2°W	2508	24,7	1983-2003	Hanna et al. (2006)	3	220-831 (529)
(8) Basin 8	2003	69.5°N 36.2°W	3015	30,2	1957-2003	Hanna et al. (2006)	8	288-555 (459)

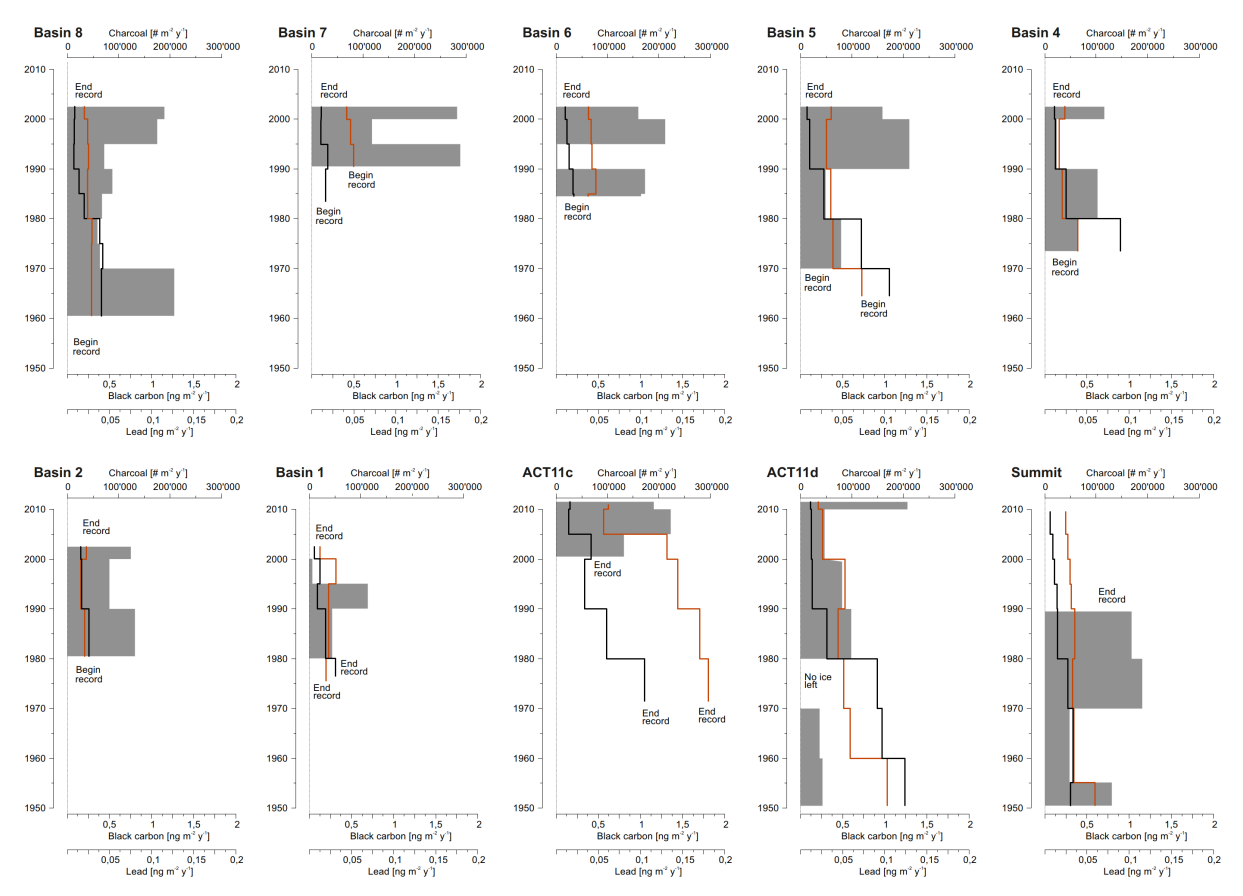


Figure 1. Comparison of 1950 to 2011 CE charcoal influx (grey bars) with black carbon (orange line) and lead (black line). Black carbon and lead values are averaged to the resolution of the charcoal records.

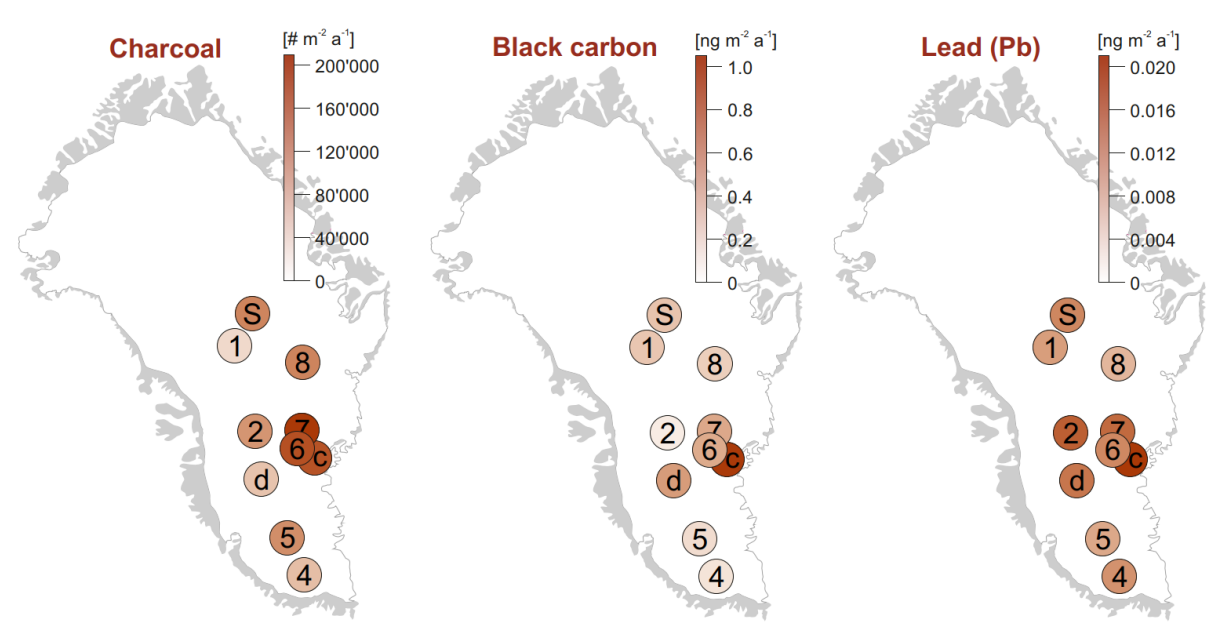


Figure 2. Deposition of charcoal, black carbon, and lead in Greenland. Shown are averages of charcoal influx over the entire length of the records weighted by the number of years contributing to each sample, and averages of black carbon and lead yearly influx for the common period 1990 to 2000 CE. See Table 1 for site codes.

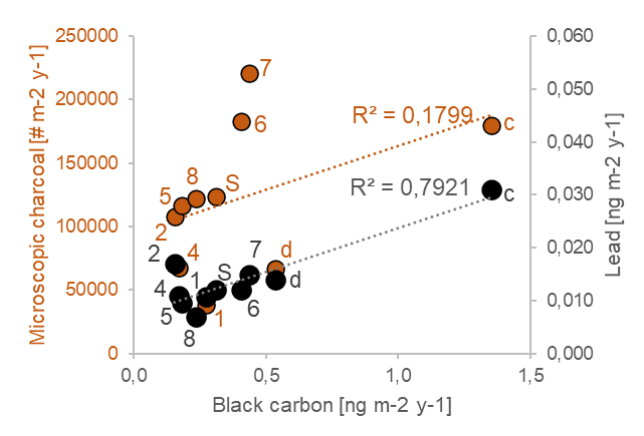


Figure 3. Correlation of black carbon deposition with microscopic charcoal (orange) and lead (black) among ice core sites. Shown are averages of charcoal influx over the entire length of the records and averages of black carbon as well as lead yearly influx for the period 1990 to 2000 CE. See Table 1 for site codes.

9 Supplementary figures

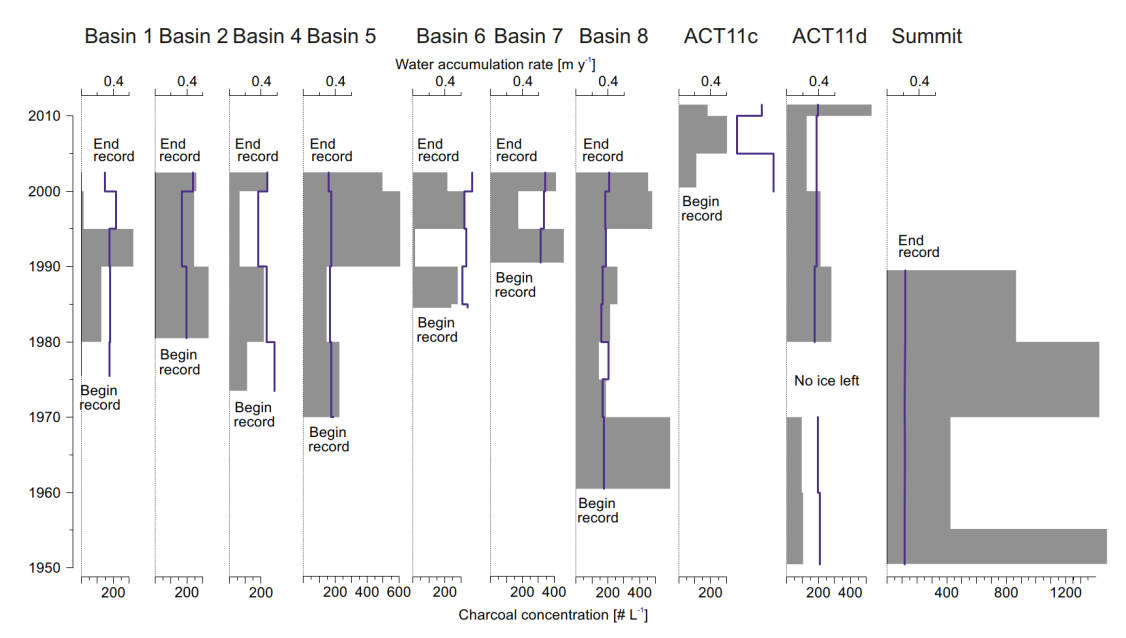


Figure S1. Charcoal concentrations in an array of shallow ice cores from Greenland (grey bars) from 1950 to 2011 CE. Blue line indicates snow accumulation in water equivalent for each sample.

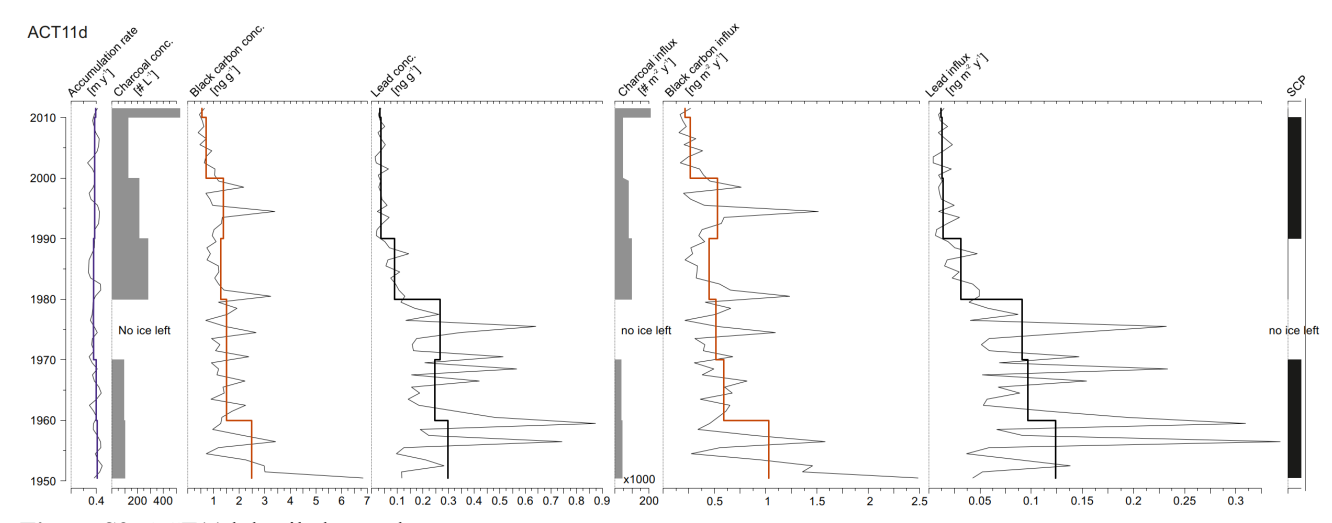


Figure S2. ACT11d detailed record.

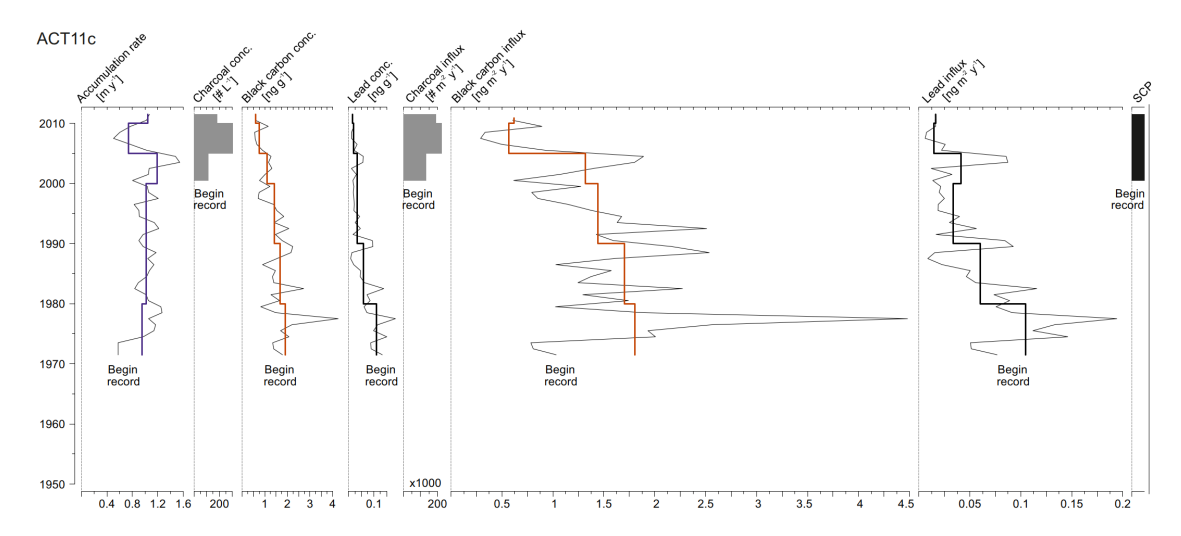


Figure S3. ACT11c detailed record.

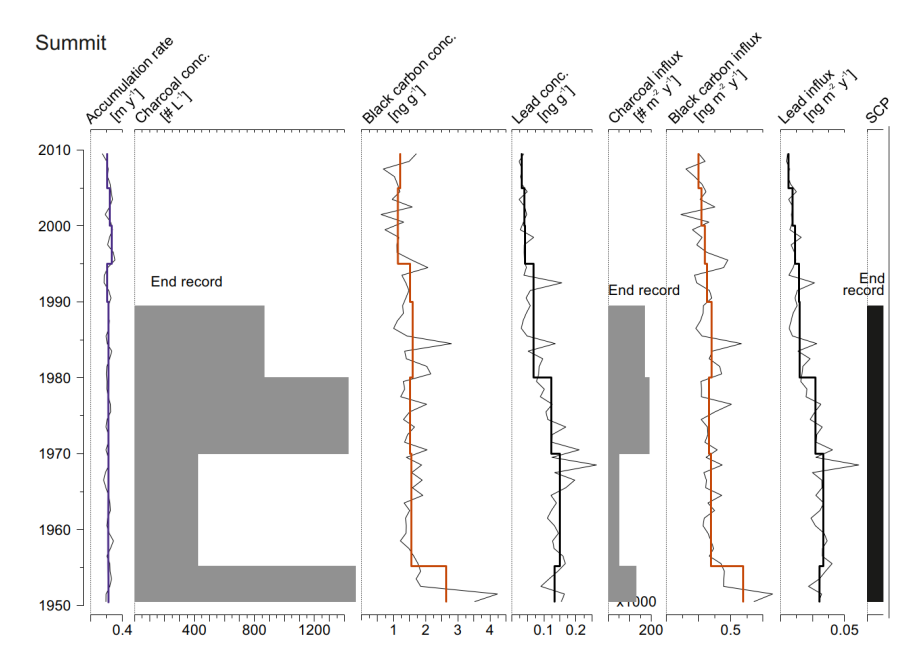


Figure S4. Summit detailed record.

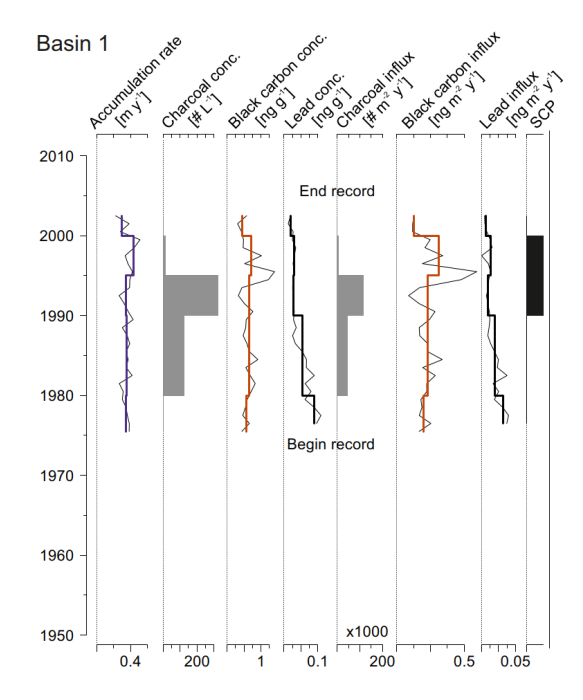


Figure S5. Basin 1 detailed record.

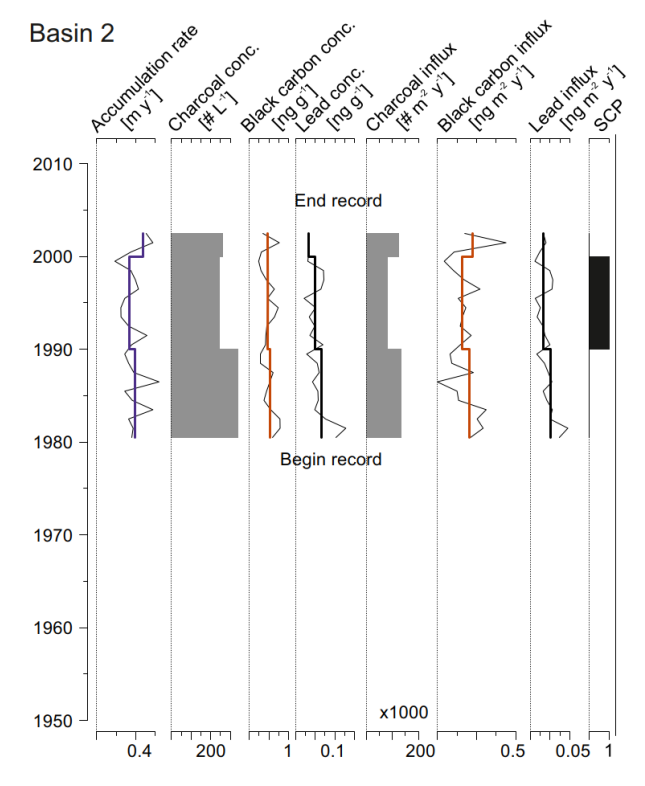


Figure S6. Basin 2 detailed record.

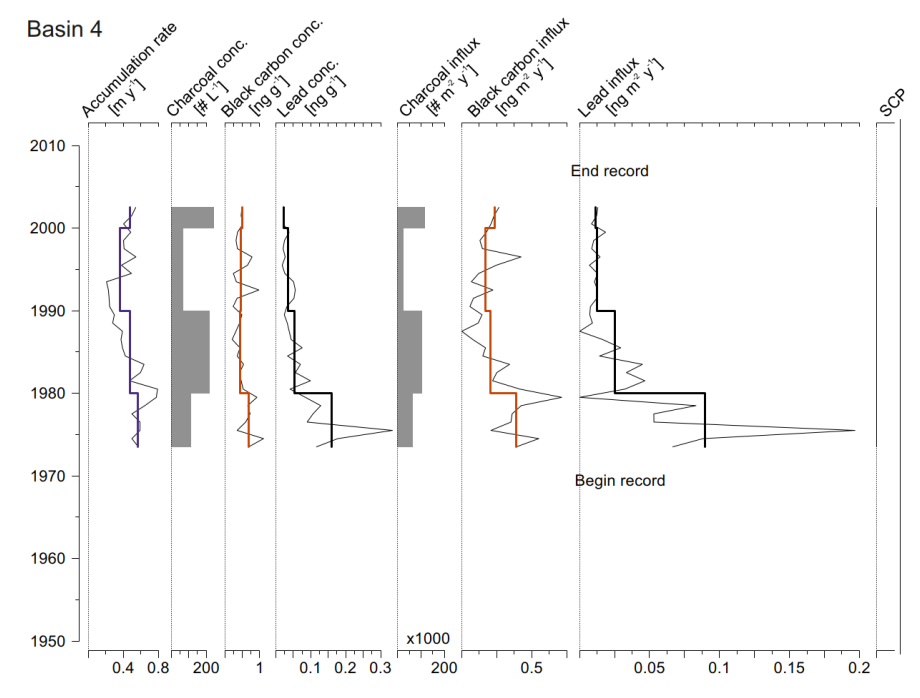


Figure S7. Basin 4 detailed record.

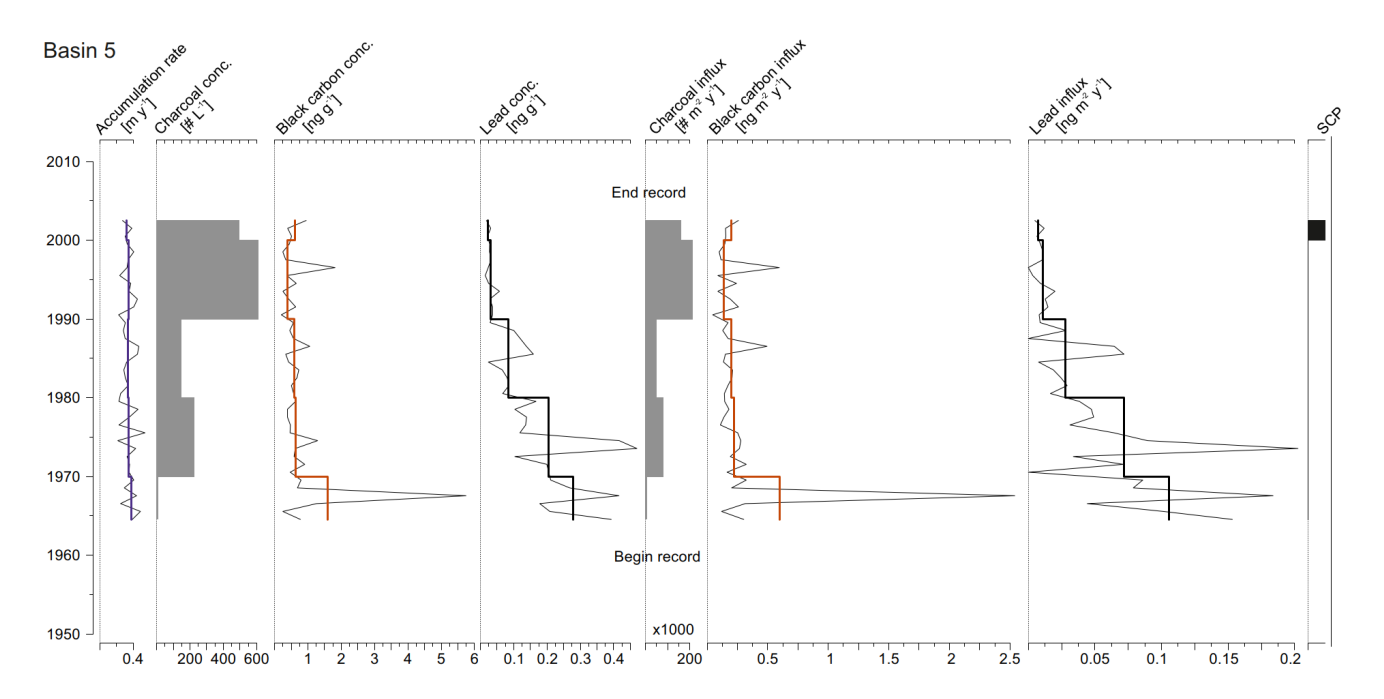


Figure S8. Basin 5 detailed record.

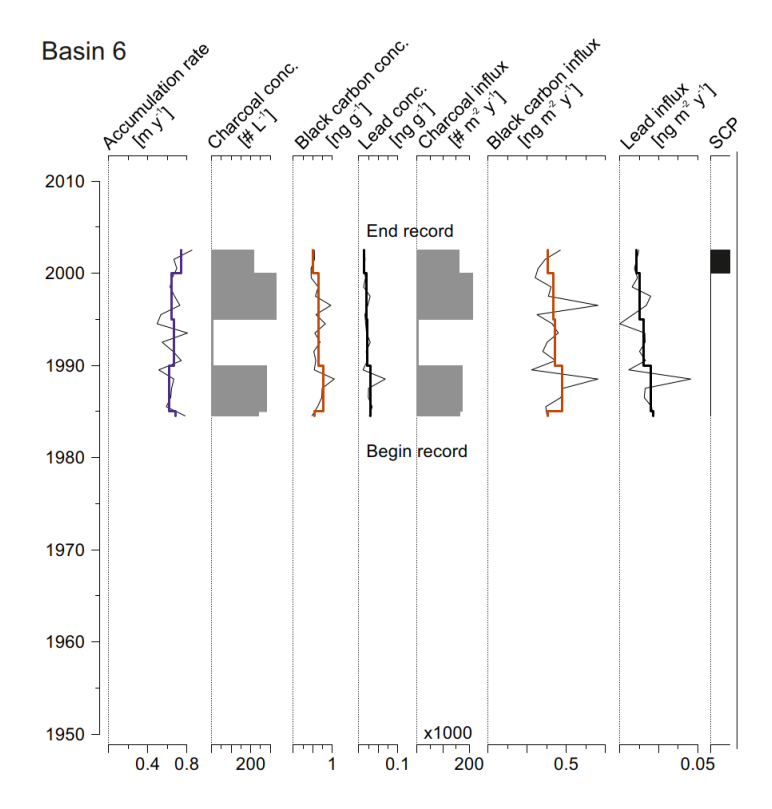


Figure S9. Basin 6 detailed record.

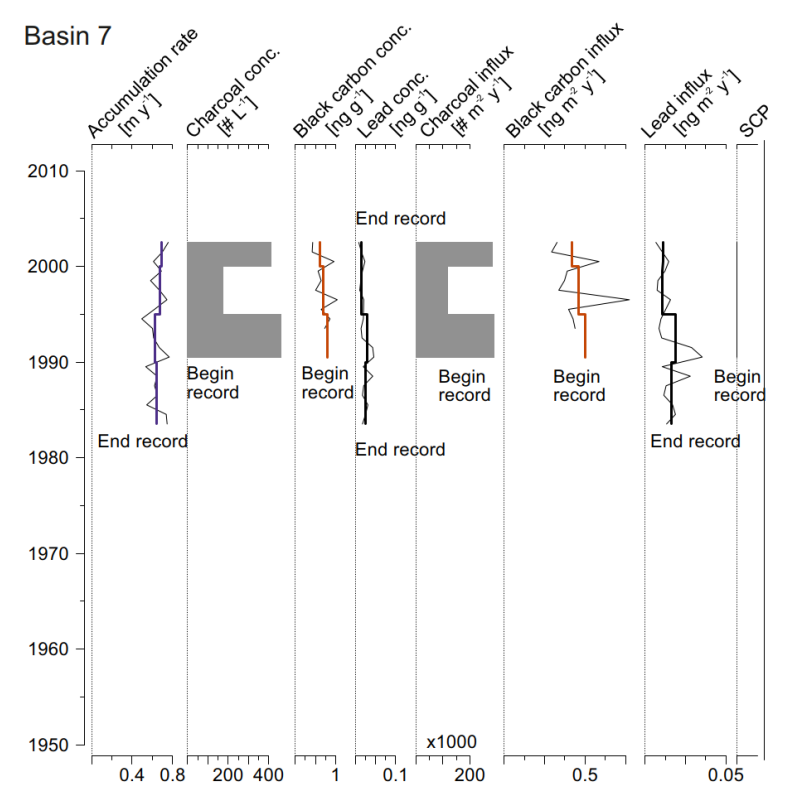


Figure S10. Basin 7 detailed record.

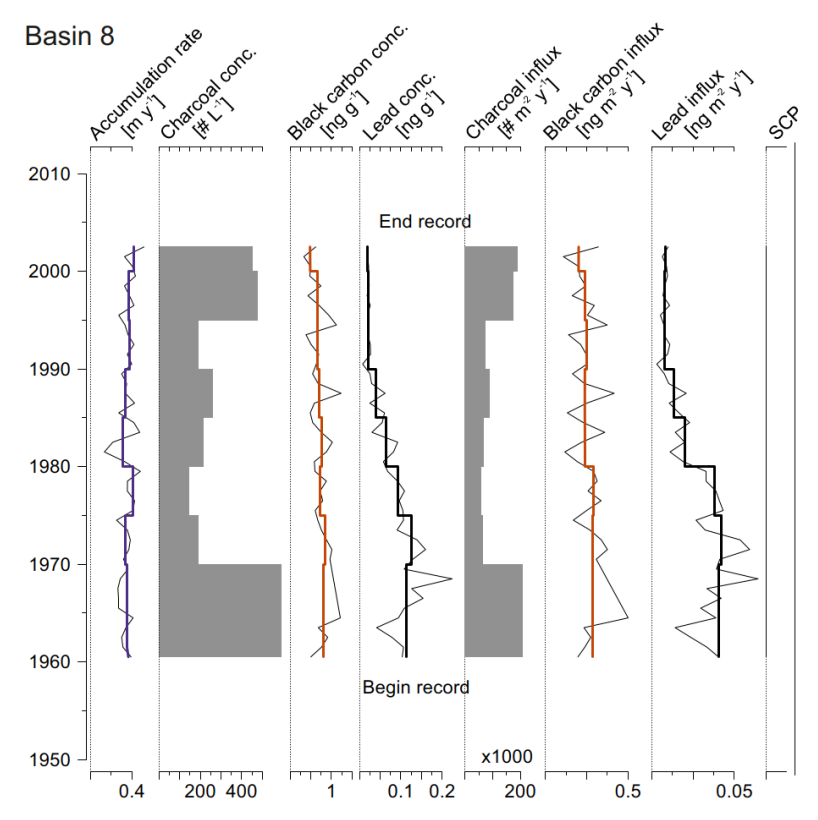


Figure S11. Basin 8 detailed record.